Trans. Phenom. Nano Micro Scales, 5(2): 102-110, Summer and Autumn 2017
DOI: 10.7508/tpnms.2017.02.004

ORIGINAL RESEARCH PAPER

Numerical simulation of nanofluid flow over diamond-shaped elements in tandem in laminar and turbulent flow

Hamed Safikhani[1,2,*], Ebrahim Hajian[3], Rafat Mohammadi[1]

[1]*Department of Mechanical Engineering, Faculty of Engineering, Arak University, Arak 38156-88349, Iran*
[2]*Institue of Nanosciences & Nanotechnolgy, Arak University, ARAK, I. R. IRAN*
[3]*Department of Mechanical Engineering, Iran University of Science and Technology (IUST), Narmak, Tehran 16844, Iran*

Received 28 March 2016; revised 24 November 2016; accepted 29 November 2016; available online 10 June 2017

ABSTRACT: In this paper, the Al_2O_3-water nanofluid flow in laminar and turbulent flows inside tubes fitted with diamond-shaped turbulators is numerically modeled. The nanofluid flow is modeled by employing a two-phase mixture method and applying the constant heat flux boundary condition at tube walls. In the results, the effects of different parameters such as the geometry of turbulators, volume fraction and diameter of nanoparticles, etc. on the flow field in the tubes have been investigated. The obtained results indicate that, with the reduction of tail length ratio (*TR*) and increase of vertex angle of turbulators (θ), the heat transfer coefficient as well as the wall shear stress increase. Similarly, with the reduction of TR and increase of θ, the amount of secondary flows, vortices and the turbulent kinetic energy increase. Moreover, the increase in the volume fraction of nanoparticles and the reduction of nanoparticles diameter lead to the increase of the heat transfer coefficient and wall shear stress.

KEYWORDS: *Nanofluid; Diamond-shaped turbulators; CFD; Turbulent flow; Mixture model*

INTRODUCTION

Increasing the amount of heat transfer in different engineering applications such as the cooling of electronic components, cooling and boiling of liquids, design and operation of heat exchangers, etc. is highly important. The methods of heat transfer improvement can be generally divided into two groups of active and passive techniques. The passive heat transfer enhancement method, due to its simplicity of use and lower cost, has greatly attracted the attention of industrialists and researchers in recent years [1-6].

A very important and useful way of passively increasing the amount of heat transfer is the use of turbulators in flow passage to induce and promote the flow turbulence and to increase the local Reynolds number. In this regard, numerous investigations have been conducted in recent years both numerically and experimentally. Eiamsa-ard and Promvonge [1] experimentally studied the flow of air in circular tubes fitted with diamond-shaped turbulators. They explored the effects of the tail length ratio and also the vertex angle of the diamond-shaped turbulators on the heat transfer coefficient and the friction factor of the fluid. Ayhan et al. [2] experimentally and numerically investigated the increase in the amount of heat transfer in circular tubes containing truncated hollow cone turbulators. Durmus [3] evaluated the improvement of heat transfer in 4 different cut out conical turbulators.

✉ *Corresponding Author Email: *h-safikhani@araku.ac.ir*
Tel.: 09120686211; Note. This manuscript was submitted on March 28, 2016; approved on November 24, 2016; published online June 10, 2017.

He compared the heat transfer coefficient, pressure drop and exergy values obtained with and without the use of turbulators. Eiamsa-ard and Promvonge [4] investigated the improvement of heat transfer in tubes fitted with V-shaped turbulators. They demonstrated that these turbulators can increase the amount of heat transfer by 270% relative to flows in ordinary circular tubes. Promvonge [5] studied the effects of different diameters and arrangements of conical turbulators in fluid flows on the heat transfer and friction coefficient values of tubes. Akansu [6] numerically investigated the characteristics of fluid flow in tubes containing porous rings and demonstrated that the highest amount of heat transfer is obtained at the ratio of $H/d = 2$.

Another technique for enhancing the heat transfer in tubes is the use of a nanofluid instead of base fluid. A nanofluid refers to a compound in which solid, and mostly metallic, particles at nano sizes (usually less than 100 *nm*) are added to an ordinary fluid and help increase the value of the mixture conductivity and thus improve the amount of heat transfer in that fluid. Due to a considerable improvement of heat transfer and a negligible pressure drop achieved by nanofluids, relative to ordinary fluids, the use of nanofluids has become very commonplace in recent years [7-10]. Also in recent years, the combined use of nanofluids in conjunction with other heat transfer improvement mechanisms such as twisted tapes and coiled wires has been on the rise [11-12]. Nevertheless, based on our information, no research has been conducted so far on the subject of nanofluid flow in tubes containing diamond-

Nomenclature

a	Acceleration (m s^{-2})
C_p	Specific heat (J kg^{-1} K^{-1})
C	Constant in Eq. (14)
d_p	Diameter of nanoparticles (m)
g	Gravitational acceleration (m s^{-2})
h	Local heat transfer coefficient (W/m^2K)
k	Thermal conductivity (W m^{-1} K^{-1})
k_B	Boltzmann constant (=1.3807 × 10-23 J K^{-1})
L	Length of tubes (m)
L_h	Head length of turbulator (m)
L_t	Tain length of turbulator (m)
Pr	Prandtl number (=α_m/ν_m)
q"	Heat flux (W m^{-2})
Re	Reynolds number (=VD_h/ν_m)
T	Temperature (K)
TR	Tail length ratio (=l_t/l_h)
V	Velocity (m s^{-1})

Greek Symbols

β	Volumetric expansion coefficient (K^{-1})
δ	Distance between particles (m)
Φ	Nanoparticles volume fraction
θ	Semi vertex angle of turbulators
λ_f	Mean free path of water molecular (m)
μ	Dynamic viscosity (N s m^{-2})
ν	Kinematic viscosity (m^2 s^{-1})

Subscripts

BF	Base fluid
dr	Drift
f	Fluid
i	Inlet conditions
k	Indices
m	Mixture
p	Nanoparticle phase
w	Wall
α	Thermal diffusivity (=$k/\rho c_p$)

shaped turbulators. In this paper, the effects of simultaneously applying two heat transfer enhancement mechanisms, namely, the use of nanofluids and also diamond-shaped turbulators in laminar and turbulent flows have been numerically investigated.

MATHEMATICAL MODELING

Geometry

The geometries evaluated in this paper include different circular tubes fitted with diamond-shaped turbulators. Figure 1 shows the schematic of these tubes. The effects of different geometrical parameters such as *TR* and θ on the behavior of nanofluid flow will be investigated in this paper. The results will be obtained and displayed for 3 different *TR* and 3 different θ values.

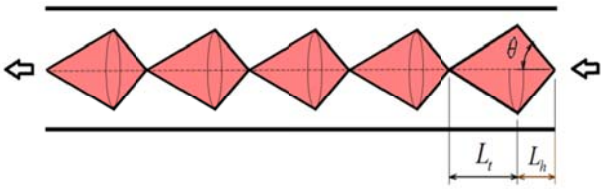

Fig.1. Detailed definition of diamond-shaped turbulators in tube

Governing equations

In the present study, numerical simulation of nanofluid flow is performed using mixture model which is a single fluid two phase approach. This method investigates equilibrium over spatial length scales. In this method each phase has its own velocity field, and in a given control volume there is a certain fraction of base fluid and nanoparticles.

Instead of utilizing the governing equations of each phase separately, it solves the continuity, momentum and energy equations for the mixture, and the volume fraction equation for nanoparticles. The equations for the steady state conditions and turbulent mean flow are as follows:

Continuity:

$$\nabla.(\rho_m V_m) = 0 \tag{1}$$

Momentum:

$$\nabla.(\rho_m V_m V_m) = -\nabla p_m + \nabla.(\tau - \tau_t) + \nabla.(\sum_{k=1}^{n} \varphi_k \rho_k V_{dr,k} V_{dr,k}) + \rho_m g \tag{2}$$

Energy:

$$\nabla.(\sum_{k=1}^{n} \rho_k C_{pk} \varphi_k V_k T) = \nabla.(k_m \nabla T - \rho_m C_{pm} \overline{vt}) \tag{3}$$

Volume fraction:

$$\nabla.(\phi_P \rho_P V_m) = -\nabla.(\phi_P \rho_P V_{dr,P}) \tag{4}$$

Where V_m is the mass average velocity:

$$V_m = \frac{\sum_{k=1}^{n} \phi_k \rho_k V_k}{\rho_m} \tag{5}$$

In Equation 2, $V_{dr,k}$ is the drift velocity for nanoparticles:

$$V_{dr,k} = V_k - V_m \tag{6}$$

The slip velocity (relative velocity) is calculated as the velocity of nanoparticles relative to the velocity of base fluid:

$$V_{pf} = V_p - V_f \tag{7}$$

The relation between drift velocity and relative velocity is as follows:

$$V_{dr,p} = V_{pf} - \sum_{k=1}^{n} \frac{\phi_k \rho_k}{\rho_m} V_{fk} \tag{8}$$

The relative velocity and drag function are calculated using Manninen et al. [13] and Schiller and Naumann [14] relations respectively, as follows:

$$V_{pf} = \frac{\rho_P d_P^2}{18 \mu_f f_{drag}} \frac{(\rho_P - \rho_m)}{\rho_P} a \tag{9}$$

$$f_{drag} = \begin{cases} 1 + 0.15\,\mathrm{Re}_P^{0.687} & for \quad \mathrm{Re}_P \le 1000 \\ 0.0183\,\mathrm{Re}_P & for \quad \mathrm{Re}_P > 1000 \end{cases} \tag{10}$$

The acceleration (a) in Eq. (9) is

$$a = g - (V_m . \nabla) V_m \tag{11}$$

The shear stress relation is given by:

$$\tau = \mu_m \nabla V_m \tag{12}$$

$$\tau_t = \sum_{k=1}^{n} \rho_k \phi_k v_k \overline{v_k v_k} \tag{13}$$

Turbulence modeling

In this paper, as suggested by Namburu et al. [15], the *k-ε* model, proposed by Launder and Spalding [16], is investigated. This model introduces two new equations, one for the turbulent kinetic energy (*k*) and the other for turbulent dissipation rate (*ε*). The two equations are given by:

$$\nabla . (\rho_m V_m k) = \nabla . \left[(\mu_m + \frac{\mu_{tm}}{\sigma_k}) \nabla k \right] + G_m - \rho_m \varepsilon \tag{14}$$

$$\nabla . (\rho_m V_m \varepsilon) = \nabla . \left[(\mu_m + \frac{\mu_{tm}}{\sigma_\varepsilon}) \nabla \varepsilon \right] + \frac{\varepsilon}{k} (C_1 G_m - C_2 \rho_m \varepsilon) \tag{15}$$

Where

$$\mu_{tm} = \rho_m C_\mu \frac{k^2}{\varepsilon} \tag{16}$$

$$G_m = \mu_{tm} (\nabla V_m + (\nabla V_m)^T) \tag{17}$$

With C_1=1.44, C_2=1.92, C_μ=0.09, σ_K=1, σ_ε=1.

Nanofluid mixture properties

In this paper the properties of Al_2O_3-water nanofluid are calculated using the following expressions:

Density [17] :

$$\rho_m = \phi \rho_p + (1 - \phi) \rho_f \tag{18}$$

Specific heat capacity [18]:

$$(\rho C_p)_m = \phi (\rho C_p)_p + (1 - \phi)(\rho C_p)_f \tag{19}$$

Dynamic viscosity [19] :

$$\mu_m = \mu_f + \frac{\rho_p V_B d_p^2}{72 C \delta} \tag{20}$$

Where V_B and δ are the Brownian motion of nanoparticles and the distance between nanoparticles respectively and are calculated based on:

$$V_B = \frac{1}{d_p} \sqrt{\frac{18 k_B T}{\pi \rho_p d_p}} \tag{21}$$

$$\delta = \sqrt[3]{\frac{\pi}{6\phi}} d_p \tag{22}$$

C in Equation 14 is defined as:

$$C = \frac{(C_1 d_p + C_2)\phi + (C_3 d_p + C_4)}{\mu_f} \tag{23}$$

Where C_1, C_2, C_3 and C_4 are given as:

$$C_1 = -0.000001133\,,\ C_2 = -0.000002771$$
$$C_3 = 0.00000009\,,\ C_4 = -0.000000393 \tag{24}$$

Thermal conductivity [20]:

$$\frac{k_m}{k_f} = 1 + 64.7\varphi^{0.7460}\left(\frac{d_f}{d_p}\right)^{0.3690}\left(\frac{k_p}{k_f}\right)^{0.7476} \Pr_f^{0.9955}\,\mathrm{Re}_f^{1.2321} \quad (25)$$

Where Re_f and Pr_f can be expressed as:

$$Re_f = \frac{\rho k_B T}{3\pi\eta^2\lambda_f} \quad (26)$$

$$Pr_f = \frac{\eta}{\rho_f \alpha_f} \quad (27)$$

Where λ_f is the MFP (mean free path) of water molecular (λ_f= 0.17 nm), k_B is Boltzmann constant (k_B= 1.3807 × 10^{-23} J/K) and η can be defined by the following equation:

$$\eta = A.10^{\frac{B}{T-C}},\ A = 2.414\times10^{-5},\ B = 247.8, C = 140 \quad (28)$$

Thermal expansion coefficient [21]:

$$\beta_m = \left[\frac{1}{1+\frac{(1-\phi)\rho_f}{\phi\rho_p}\frac{\beta_p}{\beta_f}} + \frac{1}{1+\frac{\phi}{1-\phi}\frac{\rho_p}{\rho_f}}\right]\beta_f \quad (29)$$

Boundary conditions

To numerically model the nanofluid flow in circular tubes fitted with diamond-shaped turbulators, the problem is solved as an axisymmetric problem. The tube's central line is modeled as the axis and the tube walls are modeled with constant heat flux boundary condition.

At the inlets of tubes, the input flow velocity, temperature and the volume fraction of nanoparticles are specified and at the outlets, the constant pressure boundary condition is applied.

Numerical methods

The numerical simulation is performed using the finite volume method. A second order upwind method is used for the convective and diffusive terms and the SIMPLE algorithm is employed to solve the coupling between the velocity and pressure fields. To make sure that the obtained results are independent of the size and the number of generated grids, several grids with different sizes along different directions has been tested for each tube; and it has been attempted to consider for each tube the best grid, with the highest accuracy and the lowest computation cost. The examined tubes contain between 2 and 3 million elements.

Figure 2 shows a sample of grid generation for a tube containing diamond-shaped turbulators.

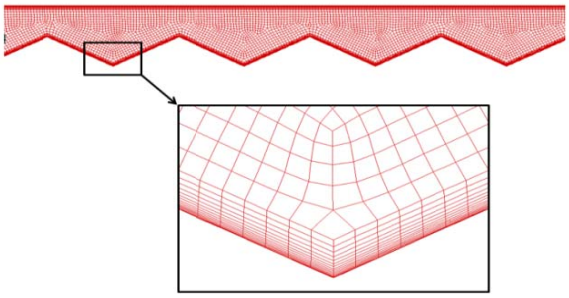

Fig. 2. A sample of grid generation

Validations

To attain the confidence about the simulations, it is necessary to compare the results with the available related data. Figures 3 and 4 compare the local heat transfer coefficient (h) in laminar and turbulent flows respectively in a plain tube of present study with the available data of Kim et al. [22] and Ebrahimnia et al. [23] (laminar flow) and Bianco et al. [24] (turbulent flow). As is evident from these figures, the present simulations agree well with the available data.

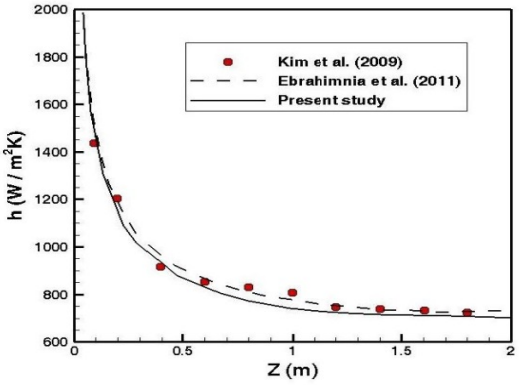

Fig.3. Comparison of local heat transfer coefficient of the present numerical simulation with the available data for laminar flow in a plain tube, Re=1460, $q'' = 2089\,{}^{W}/_{m^2}$ ، d_p=20 *nm*, Φ=3%

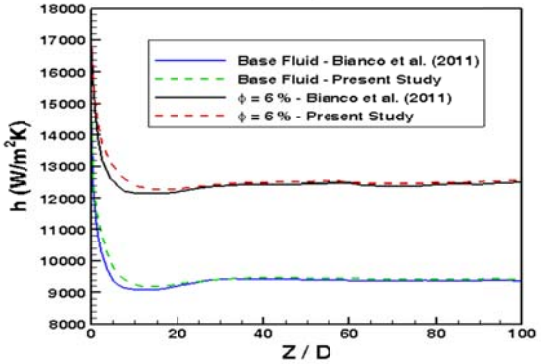

Fig. 4. Comparison of local heat transfer coefficient of the present numerical simulation with the available data for turbulent flow in a plain tube, Re=20000 ، $q'' = 500\,{}^{kw}/_{m^2}$, d_p=38 *nm*

RESULTS

In this paper, the Al_2O_3-water nanofluid flow in laminar and turbulent flows inside tubes fitted with diamond-shaped turbulators is numerically modeled. In this section, the effects of different geometrical and non-geometrical parameters on the nanofluid flow will be explored for laminar and turbulent flows in tubes. In all of the investigations, the Reynolds numbers for the laminar and turbulent flows are 1000 and 10000, respectively. Moreover in all of the investigations related to turbulent flows, parameter y^+ is controlled and it has appropriate values.

Effect of turbulator geometry

In this paper, the effects of two geometrical parameters of turbulators (*TR* and θ) on nanofluid flow field have been evaluated. Since in the flow within tubes, in addition to the amount of heat transfer, the amount of nanofluid pressure drop and thus the amount of shear stress at tube walls is also important, the latter parameter has also been investigated. Since by placing the turbulators in the way of fluid flow the shear stress of walls undergoes severe fluctuations, these shear stresses cannot be considered locally in a figure so their average values is presented in a table format. Figure 5 shows the effect of *TR* variations on the local heat transfer coefficient.

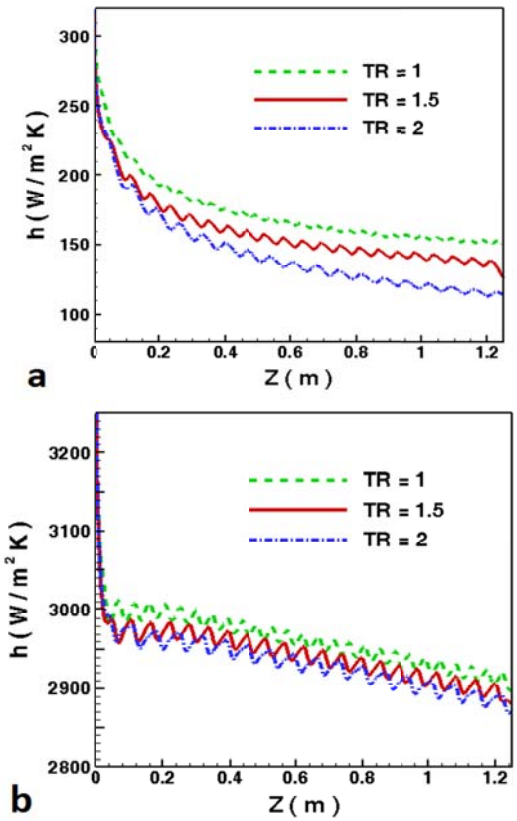

Fig. 5. Effects of tail length ratio on local heat transfer coefficient, θ=30°, $q'' = 4000\,{}^{W}/_{m^2}$, d_p=40 *nm*, *Φ=1.5%*, (a) laminar *Re*=1000 (b) turbulent *Re*=10000

Also, the impact of this parameter on the shear stress of tube walls has been presented in Table 1.

Table 1
Effect of different parameters on the average wall shear stress.

Effect of Variable	Value	τ(pa)		Changes in τ(%)	
		Laminar	Turbulent	Laminar	Turbulent
TR	1	0.047	1.23	0.00	0.00
	1.5	0.041	1.15	-12.76	-6.50
	2	0.033	0.98	-29.78	-20.32
θ(deg)	15	0.031	0.87	0.00	0.00
	22.5	0.037	1.03	19.35	18.39
	30	0.041	1.15	32.25	32.18
Φ(%)	0	0.040	1.13	0.00	0.00
	1.5	0.041	1.15	2.50	1.76
	3	0.043	1.19	7.50	5.30
d_p(nm)	20	0.41	1.14	0.00	0.00
	40	0.041	1.15	0.00	0.87

According to Figure 5, the heat transfer coefficient increases with the reduction of *TR* in both the laminar and turbulent flows. The saw tooth features in the local heat transfer coefficient diagram are due to the existence of diamond-shaped turbulators in the tube. Table 1 indicates that the reduction of *TR*, in addition to increasing the heat transfer coefficient, also increases the shear stress at the walls, which constitutes a disadvantage. As is observed, with the reduction of *TR* from 2 to 1, the wall shear stresses in laminar and turbulent flows increase by 29% and 20%, respectively. The contours of turbulent kinetic energy and the stream lines in turbulent flow have been illustrated in Figure 6 for different *TR* values. As is indicated in this figure, with the reduction of *TR*, the secondary flows and the vortices existing in flow and also the amount of turbulent kinetic energy increase. By simultaneously considering the results of these two figures, it can be concluded that the reduction of *TR* ultimately causes the heat transfer coefficient to increase by increasing the secondary flows, vortices and mixing of flow.

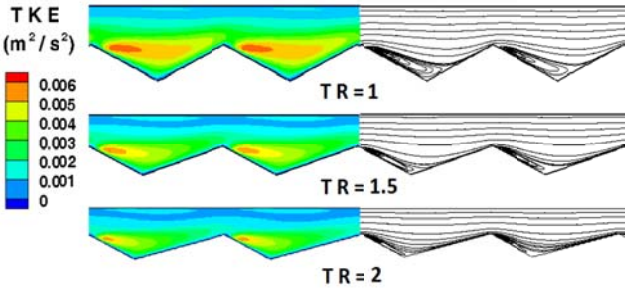

Fig. 6. Effects of tail length ratio on turbulent kinetic energy (*k*) and stream lines

Similarly, the effect of θ on the local heat transfer coefficient has been depicted in Figure 7. As is observed, by increasing the value of θ in both laminar and turbulent flows, the heat transfer coefficient can be increased. According to Table 1, the increase of θ also leads to the

increase of shear stress at the walls. With the increase of θ from 15° to 30°, the amount of wall shear stress in both the laminar and turbulent flows increases by about 32%.

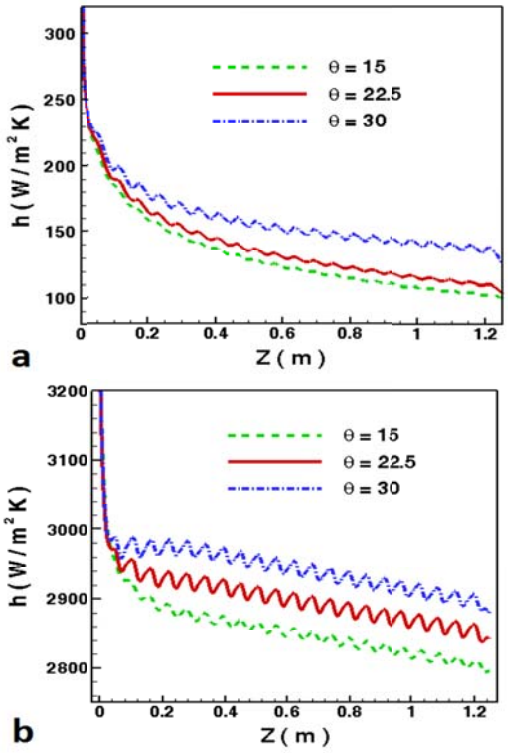

Fig. 7. Effects of vertex angle on local heat transfer coefficient, TR=1.5, $q'' = 4000\,{}^{W}/_{m^2}$, d_p=40 *nm*, Φ=*1.5%*, (a) laminar *Re*=1000 (b) turbulent *Re*=10000

The contours of turbulent kinetic energy and the stream lines in a turbulent flow are illustrated in Figure 8 for different θ values.

According to this figure, with the increase of θ, the secondary flows and the vortices existing in flow and also the amount of turbulent kinetic energy increase. Thus, it can be concluded that the increase of θ ultimately causes the heat transfer coefficient to increase by increasing the existing secondary flows and vortices in flow.

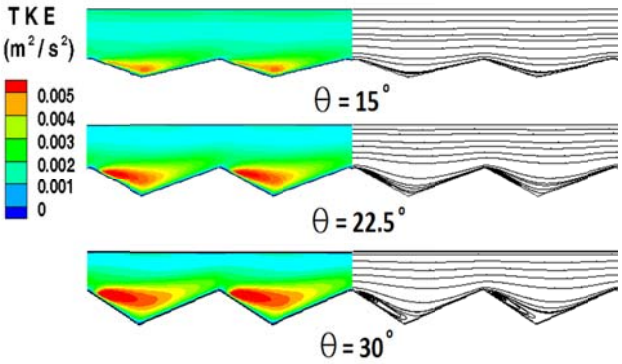

Fig. 8. Effects of vertex angle on turbulent kinetic energy (*k*) and stream lines

Effect of nanoparticle parameters

In this section, the effects of volume fraction and nanoparticle diameter on fluid flow in tubes fitted with diamond-shaped turbulators are investigated. Figure 9 illustrates the effect of volume fraction (as it changes from 0-3%) on the local heat transfer coefficient in laminar as well as turbulent flows. As is observed, with the increase of volume fraction from 0% to 3%, the local heat transfer coefficient increases rather significantly. Also, the third column in Table 1 indicates that with this increase in the volume fraction of nanoparticles, the amount of wall shear stress in laminar and turbulent flows increases by about 7.5 and 5.3%, respectively.

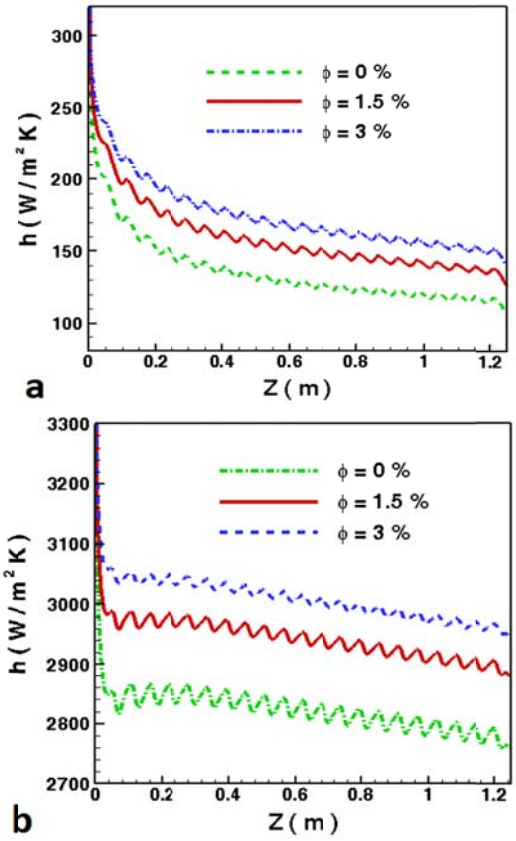

Fig. 9. Effects of nanoparticles volume fraction on local heat transfer coefficient, TR=1.5, θ=30°, $q'' = 4000\,{}^{W}/_{m^2}$ ،d_p=40 *nm*, (a) laminar *Re*=1000 (b) turbulent *Re*=10000

Figure 10 shows the effect of nanoparticle diameter (as it changes from 20-40 nm) on the local heat transfer coefficient in laminar as well as turbulent flows. As is observed, with the reduction of nanoparticle diameter from 100 to 20 *nm*, the local heat transfer coefficient increases rather considerably.

Also, the fourth column in Table 1 indicates that with the change of nanoparticle diameter, the amount of wall shear stress increases very slightly (2.43% in laminar flows and 1.75% in turbulent flows).

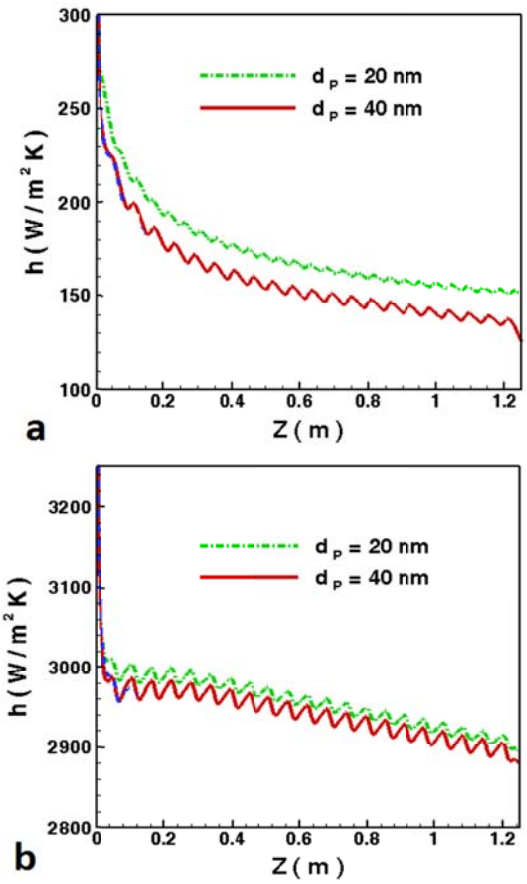

Fig. 10. Effects of nanoparticles diameter on local heat transfer coefficient, TR=1.5, θ=30°, $q'' = 4000\ ^{W}/_{m^2}$, *Φ=1.5%*, (a) laminar *Re*=1000 (b) turbulent *Re*=10000

Variations of different parameters on diamond-shaped turbulators wall Knowing how the different parameters vary on a turbulator wall can be useful in thermally designing of turbulators. The amounts of local shear stress at the wall of turbulator in laminar as well as turbulent flows have been shown in Figure 11.

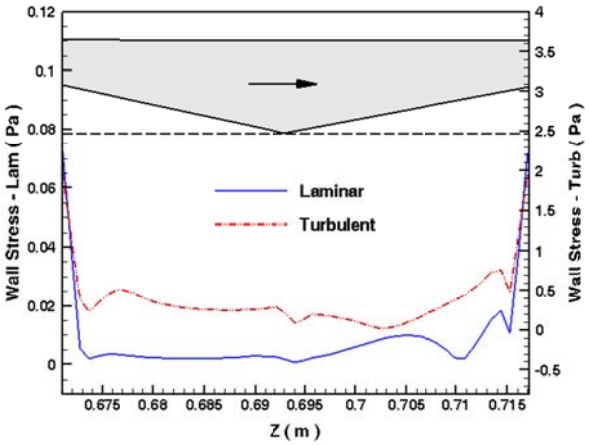

Fig. 11. Wall stress distribution across one diamond-shaped turbulators

According to this figure, the amounts of wall shear at the bulges (peaks) of the turbulators display severe changes, which cause this type of turbulators to have a considerable pressure loss. The details of the fluctuations of turbulent kinetic energy (k) and turbulent dissipation rate (ε) on turbulator wall have been shown in Figure 12. As is observed, the changes of both parameters are qualitatively similar and the maximum and minimum amounts of these parameters respectively appear at the peaks (bulges) and valleys (dents).

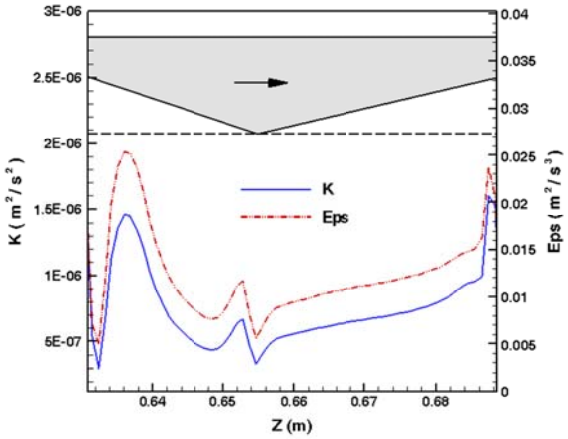

Fig. 12. Turbulent kinetic energy (k) and turbulent dissipation rate (ε) distributions across one diamond-shaped turbulators.

The changes of pressure over turbulator wall in laminar and turbulent flow regimes have been depicted in Figure 13. According to this figure, nanofluid has the least amount of pressure at the peaks.

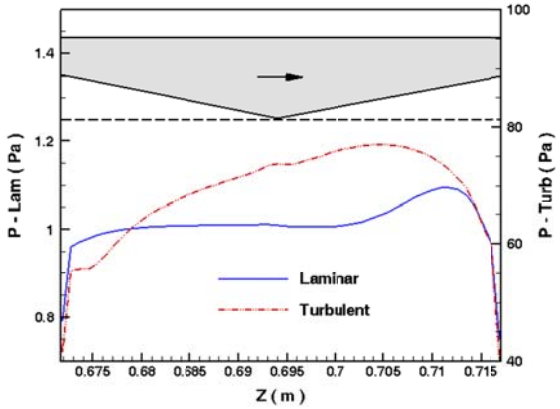

Fig. 13. Pressure distribution across one diamond-shaped turbulators

CONCLUSION

In this paper, the flow field of Al_2O_3-water nanofluid in laminar and turbulent flows inside tubes containing diamond-shaped turbulators was numerically modeled. The modeling of nanofluid was performed by employing the two-phase mixture method and applying the constant heat flux boundary condition at tube walls. The effects of

different parameters such as the geometry of turbulators (TR and θ), volume fraction and diameter of nanoparticles, etc. on the flow field of nanofluid in the tubes were investigated. It was observed that, with the reduction of TR and increase of θ, the amounts of heat transfer coefficient as well as the wall shear stress increase. Similarly, with the reduction of TR and increase of θ, the number of secondary flows, vortices and turbulent kinetic energy in the flow increase. Also, the increase in the volume fraction of nanoparticles and the reduction of the nanoparticles diameter resulted in the increase of the heat transfer coefficient and wall shear stress. Moreover, the changes of shear stress, k and ε on turbulators were investigated and it was observed that the mentioned parameters have their highest values at the hills and their lowest values at the valleys of turbulators wall.

ACKNOWLEDGEMENTS

The authors would like to acknowledge the Arak university fund for financial supporting of the project.

REFERENCES

[1] Eiamsa-ard S, Promvonge P. Thermal characterization of turbulent tube flows over diamond-shaped elements in tandem. International Journal of Thermal Sciences. 2010 Jun 30;49(6):1051-62.

[2] Ayhan T, Azak Y, Demirtas C, Ayhan B. Numerical and experimental investigation of enhancement of turbulent flow heat transfer in tubes by means of truncated hollow cone inserts. InHeat Transfer Enhancement of Heat Exchangers 1999 (pp. 347-356). Springer Netherlands.

[3] Durmuş A. Heat transfer and exergy loss in cut out conical turbulators. Energy Conversion and Management. 2004 Mar 31;45(5):785-96.

[4] Eiamsa-ard S, Promvonge P. Experimental investigation of heat transfer and friction characteristics in a circular tube fitted with V-nozzle turbulators. International Communications in Heat and Mass Transfer. 2006 May 31;33(5):591-600.

[5] Promvonge P. Heat transfer behaviors in round tube with conical ring inserts. Energy Conversion and Management. 2008 Jan 31;49(1):8-15.

[6] Akansu SO. Heat transfers and pressure drops for porous-ring turbulators in a circular pipe. Applied Energy. 2006 Mar 31;83(3):280-98.

[7] Putra N, Thiesen P, Roetzel W. Temperature dependence of thermal conductivity enhancement for nanofluids. J Heat Transf. 2003;125:567-74.

[8] Murshed SM,Leong KC, Yang C. A combined model for the effective thermal conductivity of nanofluids. Applied Thermal Engineering. 2009 Aug 31;29(11):2477-83.

[9] Teng TP, Hung YH, Teng TC, Mo HE, Hsu HG. The effect of alumina/water nanofluid particle size on thermal conductivity. Applied Thermal Engineering. 2010 Oct 31;30(14):2213-8.

[10] Safikhani H, Abbassi A. Effects of tube flattening on the fluid dynamic and heat transfer performance of nanofluids. Advanced Powder Technology. 2014 May 31;25(3):1132-41.

[11] Eiamsa-ard S, Kiatkittipong K. Heat transfer enhancement by multiple twisted tape inserts and TiO_2/water nanofluid. Applied Thermal Engineering. 2014 Sep 5;70(1):896-924.

[12] Saeedinia M, Akhavan-Behabadi MA, Nasr M. Experimental study on heat transfer and pressure drop of nanofluid flow in a horizontal coiled wire inserted tube under constant heat flux. Experimental Thermal and Fluid Science. 2012 Jan 31;36:158-68.

[13] Manninen M, Taivassalo V, Kallio S. On the mixture model for multiphase flow.

[14] Schiller VL. A drag coefficient correlation. Z. Vereines Ingenieure. 1933;77:318-20.

[15] Namburu PK, Das DK, Tanguturi KM, Vajjha RS. Numerical study of turbulent flow and heat transfer characteristics of nanofluids considering variable properties. International Journal of Thermal Sciences. 2009 Feb 1;48(2):290-302.

[16] Launder BE, Spalding DB. Lectures in mathematical models of turbulence.

[17] Pak BC, Cho YI . Hydrodynamic and heat transfer study of dispersed fluids with submicron metallic oxide particles. Experimental Heat Transfer an International Journal. 1998 Apr 1;11(2):151-70.

[18] Xuan Y, Roetzel W. Conceptions for heat transfer correlation of nanofluids. International Journal of heat and Mass transfer. 2000 Oct 1;43(19):3701-7.

[19] Masoumi N, Sohrabi N, Behzadmehr A. A new model for calculating the effective viscosity of nanofluids. Journal of Physics D: Applied Physics. 2009 Feb 9;42(5):055501.

[20] Chon CH, Kihm KD, Lee SP, Choi SU. Empirical correlation finding the role of temperature and particle size for nanofluid (Al 2 O 3) thermal conductivity enhancement. Applied Physics Letters. 2005 Oct 10;87(15):153107.

[21] Khanafer K , Vafai K , Lightstone M. Buoyancy - driven heat transfer enhancement in a two-dimensional enclosure utilizing nanofluids. International journal of heat and mass transfer. 2003 Sep 30;46(19):3639-53.

[22] Kim D, Kwon Y, Cho Y, Li C, Cheong S, Hwang Y, Lee J, Hong D, Moon S. Convective heat transfer characteristics of nanofluids under laminar and turbulent flow conditions. Current Applied Physics. 2009 Mar 31;9(2):e119-23.

[23] Ebrahimnia-Bajestan E,Niazmand H, Duangthongsuk W, Wongwises S. Numerical investigation of effective parameters in convective heat transfer of nanofluids flowing under a laminar flow regime.

International journal of heat and mass transfer. 2011 Sep 30;54(19):4376-88.

[24] Bianco V, Manca O, Nardini S. Numerical investigation on nanofluids turbulent convection heat transfer inside a circular tube. International Journal of Thermal Sciences. 2011 Mar 31;50(3):341-9.